

Ab Initio calculation of band gap renormalization in highly excited GaAs

Catalin D. Spataru,^{1,2} Lorin X. Benedict,³ and Steven G. Louie^{1,2}

¹*Department of Physics, University of California at Berkeley, Berkeley, California 94720*
²*Materials Sciences Division, Lawrence Berkeley National Laboratory, Berkeley, California 94720*
³*H Division, Physics and Advanced Technologies Directorate,*

Lawrence Livermore National Laboratory, University of California, Livermore, CA 94550

(Dated: October 30, 2018)

We present *ab initio* quasiparticle self-energy calculations in crystalline GaAs for cases of intense electronic excitation ($\sim 10\%$ of valence electrons excited into conduction band), relevant for high-intensity ultra-short pulsed laser experiments. Calculations are performed using an out-of-equilibrium generalization of the *GW* approximation based on the Keldysh Green's function approach. Our results indicate that while the quasiparticle band gap is a sensitive function of the amount of excitation, it is not possible to induce complete band gap closure in this system by purely electronic means.

PACS numbers: 78.55.Cr, 71.15.Qe, 71.10.-w, 71.55.Eq

I. INTRODUCTION

The ability to optically pump semiconductors with ultra-short pulsed lasers has led to the discovery of a host of phenomena over the past few decades¹. One of the most interesting is band gap renormalization (BGR), or a change in the quasiparticle gap of a material which occurs when electrons are redistributed in energy. The classic scenario is one in which electrons are excited from the top of the valence band to the bottom of the conduction band (in a direct-gap material such as GaAs), leaving holes behind. Though measurements of this effect are often difficult, reductions in the band gap have been inferred in the ~ 10 meV range for excited carrier densities of $\sim 10^{15} - 10^{16} \frac{e^-}{cm^3}$ ^{1,2}. Since these carrier densities are relatively small, the material remains crystalline during the duration of an optical pumping experiment. When the carriers have relaxed to the extrema of the bands, they are amenable to theoretical treatment within the effective mass approximation. The gap reduction itself is determined by calculating the quasiparticle self-energy in a screened-interaction (e.g. *GW* approximation^{3,4}) perturbation theoretic treatment^{2,5}. Extensions of these approaches which utilize *ab initio* electronic structure techniques have been applied to BGR in conditions of high doping levels, in which excess electrons (but no holes) are present⁶.

In the last few years, optical pump-probe experiments have been performed which reach carrier densities (electrons + holes) in excess of $\sim 10^{21} \frac{e^-}{cm^3}$ ⁷. In these experiments, intense short-pulsed laser irradiation of GaAs rapidly melts the material and creates a metallic amorphous state⁸. Though the non-thermal melting is a primary goal of the studies, significant amounts of optical data were recorded prior to the time at which melting is thought to occur. For these short pump-probe delay times (\sim few hundred fs), deviations of the dielectric function from its values in the unpumped state are expected to be mostly electronic in origin (the heavier ions still being close to their equilibrium lattice positions). One of us (L.X.B.) has studied the changes in optical properties that result from the blocking of transitions (Pauli blocking) and the unbinding of exciton states which may occur in such conditions⁹. However in that work, BGR was neglected.

Calculations of BGR in GaAs for these conditions of excitation have been performed by Kim et al.¹⁰ using an empirical pseudopotential technique together with a quasistatic effective mass-derived self-energy contribution. Their conclusion was that complete band gap closure would occur if $\sim 10\%$ of the electrons are excited from the top of the valence band to the bottom of the conduction band. In their theory, a significant portion of the band gap reduction is due to the change in the screened electron-ion potential that results from the excitation of free carriers, the rest being caused by the changes in the quasiparticle self-energy. The change in Hartree potential (the interaction between electrons at the mean-field level) is neglected in their approach.

In this work, we calculate BGR for laser-excited GaAs in which electrons have been excited from the top of the valence band to occupy the lowest energy states of the bottom of the conduction band. Single-particle states are taken from *ab initio* pseudopotential local density approximation (LDA) band structure calculations, and the quasiparticle self-energy is computed in the *GW* approximation (which includes dynamical screening of the electron-electron interaction)⁴. The LDA calculations are done for constrained (excited) occupation of the electronic states, so the self-consistent contribution of the Hartree term (owing to the redistribution of charge density) is included. We find, contrary to the results of Kim et al.¹⁰, that it is impossible to induce complete band gap closure by purely electronic means, assuming that the excitation is of the type described above. The reason is that the change resulting from the electrostatic (electron-ion + Hartree) terms causes the gap to increase as electrons are moved from the valence band

top (near As) to the conduction band bottom (near Ga). While our *ab initio* calculation of the self-energy contribution yields similar results to those of the more approximate theories^{2,5}, it is the electrostatic contribution which dominates the picture at high carrier density ($> 10\%$). In what follows, we describe the derivation of the self-energy contribution within the *GW* approximation using the Keldysh technique, present the details of our computation of BGR, and discuss our results.

II. THEORY AND COMPUTATION

A. Quasiparticle Self-energy Operator in the *GW* Approximation: Non-equilibrium Case

We are interested in describing the single-particle excitations of a system of interacting electrons out of equilibrium¹¹. Thus, we appeal to non-equilibrium quantum many-body theory, in particular, the Keldysh method. Using the Keldysh technique¹², Green's functions, self-energies, etc., for non-equilibrium problems can be constructed in a way similar to that for equilibrium problems. The only difference is the replacement of time-ordered Green's functions with contour-ordered Green's functions¹³:

$$G(\mathbf{r}_1, \mathbf{r}_2; \tau_1, \tau_2) = -i\langle T_C[\Psi_H(\mathbf{r}_1; \tau_1)\Psi_H^\dagger(\mathbf{r}_2; \tau_2)] \rangle, \quad (1)$$

where the time-labels lie on a contour with two branches: $\tau = t, \eta$ ($\eta = 1, 2$). (See Fig. 1.) The contour C runs along the real axis, starting from $-\infty$ on branch $\eta = 1$, passing through τ_1 and τ_2 once and returning to $-\infty$ on branch $\eta = 2$. Such a contour allows us to conduct the thought-experiment in which the system begins in some excited state of the non-interacting system, then the interactions are turned on adiabatically, turned slowly off again, and the system is returned to its initial state. This intellectual construct is necessary when relating expectation values of quantities in an interacting system to the corresponding expectation values of the non-interacting system¹⁴. In what follows, we omit the spatial variables for simplicity, which are to be used exactly as in the equilibrium case. We return to the full notation later.

The contour-ordered Green's function obeys the same Dyson equation as the time-ordered Green's function, if one replaces the real time axis integrals by contour integrals:

$$G(\tau_1, \tau_2) = G_0(\tau_1, \tau_2) + \int_C d\tau_3 \int_C d\tau_4 G_0(\tau_1, \tau_3)\Sigma(\tau_3, \tau_4)G(\tau_4, \tau_2). \quad (2)$$

We use the *GW* approximation for the self-energy:

$$\Sigma(\tau_1, \tau_2) = iG(\tau_1, \tau_2)W(\tau_1, \tau_2), \quad (3)$$

where the screened Coulomb potential W obeys the following self-consistent equation:

$$W(\tau_1, \tau_2) = V\delta(\tau_1 - \tau_2) + V \int_C d\tau_3 P(\tau_1, \tau_3)W(\tau_3, \tau_2), \quad (4)$$

where V is the Coulomb potential. The polarization function is calculated within the random phase approximation (RPA):

$$P(\tau_1, \tau_2) = -iG(\tau_1, \tau_2)G(\tau_2, \tau_1). \quad (5)$$

In order to make the calculations tractable, we replace the contour integrals by real time integrals. This is achieved using the Langreth rules for analytic continuation¹⁵, which we present in the Appendix, after introducing some commonly used notation for functions, A , defined on the contour (called 'lesser', 'greater', 'retarded' and 'advanced' respectively):

$$\begin{aligned} A^<(t, t') &\equiv A(t, \eta = 1, t', \eta' = 2) \\ A^>(t, t') &\equiv A(t, \eta = 2, t', \eta' = 1) \\ A^r(t, t') &\equiv \theta(t - t')[A^>(t, t') - A^<(t, t')] \\ A^a(t, t') &\equiv \theta(t' - t)[A^<(t, t') - A^>(t, t')]. \end{aligned} \quad (6)$$

Our goal is now to evaluate the retarded quasiparticle self-energy operator, Σ^r , in the *GW* approximation. From (3), (6), and (A.4) (see Appendix), Σ^r becomes:

$$\Sigma^r(t, t') = i[G^<(t, t')W^r(t, t') + G^r(t, t')W^<(t, t') + G^r(t, t')W^r(t, t')],$$

which can be further simplified using (A.1) and (A.2):

$$\Sigma^r(t, t') = i[G^<(t, t')W^r(t, t') + G^r(t, t')W^>(t, t')]. \quad (7)$$

The Keldysh components of the screened Coulomb interaction are found using the Langreth rule (A.3):

$$\begin{aligned} W^r(t, t') &= V\delta(t - t') + V \int_{-\infty}^{\infty} dt_1 P^r(t, t_1) W^r(t_1, t') \\ W^a(t, t') &= V\delta(t - t') + V \int_{-\infty}^{\infty} dt_1 P^a(t, t_1) W^a(t_1, t') \\ W^<(t, t') &= V \int_{-\infty}^{\infty} dt_1 [P^r(t, t_1) W^<(t_1, t') + P^<(t, t_1) W^a(t_1, t')] \\ W^>(t, t') &= V \int_{-\infty}^{\infty} dt_1 [P^r(t, t_1) W^>(t_1, t') + P^>(t, t_1) W^a(t_1, t')]. \end{aligned} \quad (8)$$

It can be shown^{16,17} that the self-consistent equations (8) lead to the following relations for the “greater” and “lesser” components of the screened interaction:

$$\begin{aligned} W^<(t, t') &= \int_{-\infty}^{\infty} dt_1 \int_{-\infty}^{\infty} dt_2 W^r(t, t_1) P^<(t_1, t_2) W^a(t_2, t') \\ W^>(t, t') &= \int_{-\infty}^{\infty} dt_1 \int_{-\infty}^{\infty} dt_2 W^r(t, t_1) P^>(t_1, t_2) W^a(t_2, t'). \end{aligned} \quad (9)$$

We construct “non-interacting” Green’s functions within the quasiparticle approximation from LDA¹⁸ Bloch wavefunctions $|n\mathbf{k}\rangle$, and eigenvalues $E_{n\mathbf{k}}$. Using (1) and (6) we find:

$$\begin{aligned} \langle n\mathbf{k}|G^r(\omega)|m\mathbf{k}'\rangle &= \frac{1}{\omega - E_{n\mathbf{k}} + i\eta} \delta_{nm} \delta_{\mathbf{k}\mathbf{k}'} \\ \langle n\mathbf{k}|G^a(\omega)|m\mathbf{k}'\rangle &= \frac{1}{\omega - E_{n\mathbf{k}} - i\eta} \delta_{nm} \delta_{\mathbf{k}\mathbf{k}'} \\ \langle n\mathbf{k}|G^<(\omega)|m\mathbf{k}'\rangle &= 2\pi i f(E_{n\mathbf{k}}) \delta(\omega - E_{n\mathbf{k}}) \delta_{nm} \delta_{\mathbf{k}\mathbf{k}'} \\ \langle n\mathbf{k}|G^>(\omega)|m\mathbf{k}'\rangle &= -2\pi i [1 - f(E_{n\mathbf{k}})] \delta(\omega - E_{n\mathbf{k}}) \delta_{nm} \delta_{\mathbf{k}\mathbf{k}'}, \end{aligned} \quad (10)$$

where $\eta = 0^+$ and we assumed that the “non-interacting” system can be characterized by a distribution function in energy, $f(E)$.

In frequency space, the expression for the retarded self-energy (7) becomes:

$$\begin{aligned} \langle n\mathbf{k}|\Sigma^r(\omega)|n\mathbf{k}\rangle &= i \sum_{m, \mathbf{q}, \mathbf{G}, \mathbf{G}'} M_{\mathbf{G}}^*(n, m, \mathbf{k}, -\mathbf{q}) M_{\mathbf{G}'}(n, m, \mathbf{k}, -\mathbf{q}) \\ &\times \int_{-\infty}^{\infty} \frac{d\omega'}{2\pi} [W_{\mathbf{G}, \mathbf{G}'}^r(\mathbf{q}, \omega') G^<(\mathbf{k} - \mathbf{q}, E_{n\mathbf{k}} - \omega') + W_{\mathbf{G}, \mathbf{G}'}^>(\mathbf{q}, \omega') G^r(\mathbf{k} - \mathbf{q}, E_{n\mathbf{k}} - \omega')], \end{aligned} \quad (11)$$

where the matrix elements M are defined by: $M_{\mathbf{G}}(n, m, \mathbf{k}, -\mathbf{q}) = \langle m\mathbf{k} - \mathbf{q}|e^{-i(\mathbf{q} + \mathbf{G})\mathbf{r}}|n\mathbf{k}\rangle$. Next we need the Fourier components of the screened Coulomb interaction. Using (8) and (9), the Fourier components of the screened Coulomb interaction can be written:

$$\begin{aligned} W_{\mathbf{G}, \mathbf{G}'}^r(\mathbf{q}, \omega) &= [\epsilon^r(\mathbf{q}, \omega)^{-1}]_{\mathbf{G}, \mathbf{G}'} V(\mathbf{q} + \mathbf{G}') \\ W_{\mathbf{G}, \mathbf{G}'}^a(\mathbf{q}, \omega) &= [\epsilon^a(\mathbf{q}, \omega)^{-1}]_{\mathbf{G}, \mathbf{G}'} V(\mathbf{q} + \mathbf{G}') \\ W_{\mathbf{G}, \mathbf{G}'}^<(\mathbf{q}, \omega) &= -[\epsilon^r(\mathbf{q}, \omega)^{-1} \epsilon^<(\mathbf{q}, \omega) \epsilon^a(\mathbf{q}, \omega)^{-1}]_{\mathbf{G}, \mathbf{G}'} V(\mathbf{q} + \mathbf{G}') \\ W_{\mathbf{G}, \mathbf{G}'}^>(\mathbf{q}, \omega) &= -[\epsilon^r(\mathbf{q}, \omega)^{-1} \epsilon^>(\mathbf{q}, \omega) \epsilon^a(\mathbf{q}, \omega)^{-1}]_{\mathbf{G}, \mathbf{G}'} V(\mathbf{q} + \mathbf{G}'), \end{aligned} \quad (12)$$

where the dielectric function is defined by:

$$\begin{aligned} \epsilon_{\mathbf{G}, \mathbf{G}'}^r(\mathbf{q}, \omega) &= \delta_{\mathbf{G}, \mathbf{G}'} - V(\mathbf{q} + \mathbf{G}) P_{\mathbf{G}, \mathbf{G}'}^r(\mathbf{q}, \omega) \\ \epsilon_{\mathbf{G}, \mathbf{G}'}^a(\mathbf{q}, \omega) &= \delta_{\mathbf{G}, \mathbf{G}'} - V(\mathbf{q} + \mathbf{G}) P_{\mathbf{G}, \mathbf{G}'}^a(\mathbf{q}, \omega) \\ \epsilon_{\mathbf{G}, \mathbf{G}'}^<(\mathbf{q}, \omega) &= -V(\mathbf{q} + \mathbf{G}) P_{\mathbf{G}, \mathbf{G}'}^<(\mathbf{q}, \omega) \\ \epsilon_{\mathbf{G}, \mathbf{G}'}^>(\mathbf{q}, \omega) &= -V(\mathbf{q} + \mathbf{G}) P_{\mathbf{G}, \mathbf{G}'}^>(\mathbf{q}, \omega). \end{aligned} \quad (13)$$

The Fourier components of the polarizability are found via (5), (A.5) and (10):

$$\begin{aligned}
P_{\mathbf{G},\mathbf{G}'}^r(\mathbf{q},\omega) &= \sum_{n,m,\mathbf{p}} M_{-\mathbf{G}}^*(n,m,\mathbf{p},\mathbf{q}) M_{-\mathbf{G}'}(n,m,\mathbf{p},\mathbf{q}) \frac{f(E_{n\mathbf{p}+\mathbf{q}}) - f(E_{m\mathbf{p}})}{E_{n\mathbf{p}+\mathbf{q}} - \omega - E_{m\mathbf{p}} - i\eta} \\
P_{\mathbf{G},\mathbf{G}'}^a(\mathbf{q},\omega) &= \sum_{n,m,\mathbf{p}} M_{-\mathbf{G}}^*(n,m,\mathbf{p},\mathbf{q}) M_{-\mathbf{G}'}(n,m,\mathbf{p},\mathbf{q}) \frac{f(E_{n\mathbf{p}+\mathbf{q}}) - f(E_{m\mathbf{p}})}{E_{n\mathbf{p}+\mathbf{q}} - \omega - E_{m\mathbf{p}} + i\eta} \\
P_{\mathbf{G},\mathbf{G}'}^<(\mathbf{q},\omega) &= -2\pi i \sum_{n,m,\mathbf{p}} M_{-\mathbf{G}}^*(n,m,\mathbf{p},\mathbf{q}) M_{-\mathbf{G}'}(n,m,\mathbf{p},\mathbf{q}) f(E_{n\mathbf{p}+\mathbf{q}}) [1 - f(E_{m\mathbf{p}})] \delta(E_{n\mathbf{p}+\mathbf{q}} - \omega - E_{m\mathbf{p}}) \\
P_{\mathbf{G},\mathbf{G}'}^>(\mathbf{q},\omega) &= -2\pi i \sum_{n,m,\mathbf{p}} M_{-\mathbf{G}}^*(n,m,\mathbf{p},\mathbf{q}) M_{-\mathbf{G}'}(n,m,\mathbf{p},\mathbf{q}) [1 - f(E_{n\mathbf{p}+\mathbf{q}})] f(E_{m\mathbf{p}}) \delta(E_{n\mathbf{p}+\mathbf{q}} - \omega - E_{m\mathbf{p}}). \quad (14)
\end{aligned}$$

Decomposing the self-energy into the screened-exchange and Coulomb-hole parts⁴:

$$\langle n\mathbf{k} | \Sigma^r(E) | n\mathbf{k} \rangle = \langle n\mathbf{k} | \Sigma_{SX}^r(E) | n\mathbf{k} \rangle + \langle n\mathbf{k} | \Sigma_{CH}^r(E) | n\mathbf{k} \rangle,$$

the final expression for the retarded self-energy is:

$$\begin{aligned}
\langle n\mathbf{k} | \Sigma_{SX}^r(E) | n\mathbf{k} \rangle &= - \sum_{m,\mathbf{q},\mathbf{G},\mathbf{G}'} M_{\mathbf{G}}^*(n,m,\mathbf{k},-\mathbf{q}) M_{\mathbf{G}'}(n,m,\mathbf{k},-\mathbf{q}) \\
&\quad \times [\epsilon^r(\mathbf{q}, E - E_{m\mathbf{k}-\mathbf{q}})^{-1}]_{\mathbf{G},\mathbf{G}'} V(\mathbf{q} + \mathbf{G}') f(E_{m\mathbf{k}-\mathbf{q}}) \quad (15)
\end{aligned}$$

$$\begin{aligned}
\langle n\mathbf{k} | \Sigma_{CH}^r(E) | n\mathbf{k} \rangle &= - \sum_{m,\mathbf{q},\mathbf{G},\mathbf{G}'} M_{\mathbf{G}}^*(n,m,\mathbf{k},-\mathbf{q}) M_{\mathbf{G}'}(n,m,\mathbf{k},-\mathbf{q}) \\
\times i \int_{-\infty}^{\infty} \frac{d\omega}{2\pi} &[\epsilon^r(\mathbf{q},\omega)^{-1} \epsilon^>(\mathbf{q},\omega) \epsilon^a(\mathbf{q},\omega)^{-1}]_{\mathbf{G},\mathbf{G}'} \frac{1}{E - \omega - E_{m\mathbf{k}-\mathbf{q}} + i\eta} V(\mathbf{q} + \mathbf{G}'). \quad (16)
\end{aligned}$$

The above result represents a general expression for the self-energy (within the *GW* approximation) of a system characterized by an arbitrary distribution function, $f(E)$. In particular, in the case of a system in equilibrium at some temperature, $f(E)$ is just the Fermi distribution function, f_F , and the following holds via (13) and (14):

$$\epsilon_{\mathbf{G},\mathbf{G}'}^>(\mathbf{q},\omega) = \epsilon_{\mathbf{G},\mathbf{G}'}^<(\mathbf{q},\omega) \left[1 + \frac{1}{f_B(\omega)} \right],$$

where f_B denotes the Bose distribution function. Using this result together with the Keldysh relation (A.1) for ϵ , it can be shown that (16) becomes:

$$\begin{aligned}
\langle n\mathbf{k} | \Sigma_{CH}^r(E) | n\mathbf{k} \rangle &= - \sum_{m,\mathbf{q},\mathbf{G},\mathbf{G}'} M_{\mathbf{G}}^*(n,m,\mathbf{k},-\mathbf{q}) M_{\mathbf{G}'}(n,m,\mathbf{k},-\mathbf{q}) \\
\times \frac{1}{\pi} \int_{-\infty}^{\infty} d\omega &\frac{[\epsilon^r(\mathbf{q},\omega)^{-1} - \epsilon^a(\mathbf{q},\omega)^{-1}]_{\mathbf{G},\mathbf{G}'} (1 + f_B(\omega))}{2i} \frac{1}{E - \omega - E_{m\mathbf{k}-\mathbf{q}} + i\eta} V(\mathbf{q} + \mathbf{G}'). \quad (17)
\end{aligned}$$

For systems with inversion symmetry, we can further replace in (17) $\frac{[\epsilon^r(\mathbf{q},\omega)^{-1} - \epsilon^a(\mathbf{q},\omega)^{-1}]}{2i}$ by $Im[\epsilon^r(\mathbf{q},\omega)^{-1}]$ and thus we recover a previous result¹⁹, obtained by applying the finite temperature Matsubara Green's function formalism to a system with inversion symmetry.

B. Computational details: GaAs

We calculate the quasiparticle (QP) band-structure for crystalline GaAs in various states of electronic excitation by first order perturbation theory⁴ from the real part of the self-energy:

$$E_{n\mathbf{k}}^{QP} = E_{n\mathbf{k}} + \langle n\mathbf{k} | Re\Sigma(E_{n\mathbf{k}}^{QP}) - V_{xc} | n\mathbf{k} \rangle, \quad (18)$$

with $Re\Sigma \equiv \frac{1}{2}(\Sigma^r + \Sigma^a)$. Using $\langle n\mathbf{k} | Re\Sigma | n\mathbf{k} \rangle = Re\langle n\mathbf{k} | \Sigma^r | n\mathbf{k} \rangle$, (18) is solved by evaluating the real part of the retarded self-energy, (15) and (16), for various distribution functions f .

The ‘‘non-interacting’’ mean field wavefunctions $|n\mathbf{k}\rangle$ and eigenvalues $E_{n\mathbf{k}}$ as well as the exchange-correlation potential V_{xc} are obtained within constrained LDA performed at the experimental lattice constant. We use *ab initio*

pseudopotentials generated with the scheme of Trouiller and Martins²⁰. A plane wave basis with an energy cutoff of 30 Ry is used to represent the Bloch states. We use 50 valence plus conduction bands and discrete Monkhorst-Pack meshes²¹ of \mathbf{q} points (8x8x8) in the first BZ in the sums of (15) and (16), while crystalline local-field effects in the dielectric matrix were included by summing over \mathbf{G} , \mathbf{G}' up to a cutoff of 6 Ry. The integral over ω in (16) is evaluated by setting the integration limits to ± 50 eV.

We consider five occupation number distributions f , each corresponding to a different excited carrier density: 0%, 5%, 10%, 15% and 20% of the total number of valence electrons in the system (the coarseness of our meshes of \mathbf{q} points precludes us from considering excited carrier densities between 0% and 5%). Each is characterized by a quasi-Fermi level of the conduction bands: the energy below which all conduction states are filled. The energy above which all valence states are empty is then determined by requiring charge neutrality. Note that our assumptions imply that the individual excited electron and hole populations²² are in quasiequilibrium at $T=0$. Fig. 2 shows the excited carrier occupation in the Brillouin zone (BZ), for the various excited carrier densities considered in this work. Because the effective mass of the conduction band at Γ is very small, the Γ valley of the conduction band can accommodate less than 1% of the total number of valence electrons (n_{tot}). It follows that when the excited carrier density is several percent of n_{tot} , the excited electrons must reside in a combination of conduction Γ , L and X valleys. It is these high carrier densities that we are concerned with here, given the conditions reached in recent pump-probe experiments⁷.

III. RESULTS AND DISCUSSION

Before presenting the results of our calculations of the QP self-energy operator, we discuss the changes in the band gap caused by the excitation at the mean-field (in this case, LDA) level. Fig. 3 presents the constrained LDA calculation results of BGR. We see that the valence-conduction gap E_g^{LDA} increases linearly with the excited carrier density, the slope being only slightly smaller for the direct gap at Γ than for the indirect gaps at L and X. In order to understand these results, we analyze the dependence of the direct gap at Γ on the excited carrier density. We do this by decomposing the Kohn-Sham hamiltonian into the kinetic energy part K , the ionic potential plus the Hartree potential $V_{ion} + V_{Hartree}$, and the LDA exchange-correlation potential V_{xc} . Their individual contributions to BGR are presented in Fig. 4, which shows that the dominant term leading to the increase of the constrained LDA valence-conduction gap at Γ is the Hartree contribution. Why is the Hartree term in the band gap increasing with the excited carrier density? The answer is straightforward if we take into account that: 1) high-lying valence electrons are localized more near As, while low-lying conduction electrons are localized more near Ga. 2) under excitation the electron charge density goes from As to Ga. Then it follows that under excitation, the electrostatic energy between one electron and the total charge density goes down for valence electrons and up for conduction electrons, resulting in an increase in the valence-conduction band gap. We note that at the mean-field level, our results are different from those obtained by Kim et al.¹⁰ using a self-consistent screened empirical pseudopotential treatment. They found (for 10% excited carrier density) a significant decrease of the indirect gaps (~ 1 eV for the Γ -X gap) and no change of the direct gap at Γ . We ascribe this to their neglect of the change in the Hartree term. Though some of this mean-field effect is undoubtedly included through the screening of their pseudopotentials by the excited carriers, we suspect that a large portion of this Hartree interaction is incorrectly accounted for in their approach.

We now move to results at the QP level, by including the self-energy corrections in the GW approximation. Fig. 5 presents the main results of our work, showing that the BGR picture changes dramatically when we go from the mean-field level (constrained LDA) to the QP level: we have a substantial decrease of all band gaps for relatively low excited carrier density (less than 5%), then the band gaps are rather constant for excited carrier densities between 5% and 10%, while for relatively high excited carrier densities (larger than 10%) the band gaps increase linearly. We note that the lowest value for the renormalized gap is about 0.8 eV, which results from roughly a 10% excited carrier density and is still a direct gap at Γ .

We analyze the results of Fig. 5 by separating out the contribution from the exchange-correlation self-energy part. We do that by introducing $\delta\Sigma_g(n\%) \equiv \Sigma_g(n\%) - \Sigma_g(0\%)$ (with $\Sigma_g \equiv \langle c\mathbf{k} | Re\Sigma | c\mathbf{k} \rangle - \langle v\mathbf{k} | Re\Sigma | v\mathbf{k} \rangle$, v and c denoting the valence and conduction bands near the Fermi level, \mathbf{k} being the Γ , L or X) and we interpret $\delta\Sigma_g$ as the self-energy contribution to BGR. Fig. 6 shows the dependence of $\delta\Sigma_g$ with the excited carrier density. We see that $\delta\Sigma_g$ is negative and roughly independent of the gap we are looking at (it is largest for the indirect gap from Γ -X), and that it decreases rapidly with the excited carrier density for relatively low densities. For higher excited carrier densities, it becomes rather independent of density. It is worth noting that Kim et al. found a similar self-energy contribution for an excited carrier density of 10%: $\delta\Sigma_g(10\%) \approx -0.9$ eV (an average along the entire Γ -X direction), with the largest value at X.

There are two main sources for the self-energy contribution to BGR. One comes from the change in the Fermion occupation numbers, f , appearing explicitly in eq. (15). The other comes from the change in the electronic screening which manifests in both eqs. (15) and (16) through the dielectric function ϵ (of course, ϵ depends implicitly on f).

By increasing the excited carrier density, the screening acquires a metallic character due to the increased number of 'free' electrons in the conduction band and 'free' holes in the valence band. We find that the change in the electronic screening (affecting both the screened-exchange and the Coulomb-hole terms) accounts only for a small fraction of the BGR. For the excited carrier densities considered in this work (in excess of $3.6 \times 10^{21} \frac{e^-}{cm^3}$) the major source for the self-energy contribution to BGR was found to be the change in the Fermion occupation numbers which enter the screened-exchange self-energy expression (see the f in eq.[15]). This picture may not hold for excited carrier densities lower than $10^{21} \frac{e^-}{cm^3}$. We illustrate this observation in Fig. 7 where we show the screened-exchange self-energy contribution to the direct gap at Γ calculated in two ways: the solid line represents self-consistent calculations based on eq. (15), while the dotted line represents calculations based also on eq. (15), but in which the dielectric function ϵ^r was computed for the unexcited case. Finally, we note that our results for $\delta\Sigma_g^{SX}$ follow an approximate $\frac{1}{3}$ power law behavior in the excited carrier density; the same power law behavior for $\delta\Sigma_g^{SX}$ can be obtained employing a very simple model based on the parabolic band approximation and replacing ϵ^r with a simple dielectric constant^{5,10}.

Summarizing our results for BGR, we conclude that for relatively low excited carrier densities (up to 10% of the total valence electron density) the QP valence-conduction band gap decreases (but never closes) primarily due to the change in the Fermion occupation numbers entering the screened-exchange QP self-energy expression, while for higher excited densities the gap reaches a minimum value and undergoes an upturn with increasing density. The increase is mainly due to the change in the electrostatic energy at the mean-field level described by the Hartree term. Our prediction that there is no band gap closure due to these valence band top \rightarrow conduction band bottom excitations agrees with the measurements of L. Huang et al.⁷, in which the dielectric function of GaAs was measured at short (~ 100 fs) time delays of a pump-probe experiment and no signature of metallicity was found²³. We also mention that the approximate \mathbf{k} -independence of the BGR that we predict suggests that the overall shape of the dielectric function (i.e.- the distribution of oscillator strength in the optical absorption spectrum) in these excited configurations will be similar to that predicted by one of us⁹ using an approach in which BGR was neglected. Finally, we add that our computations of the imaginary part of the QP self-energy for the cases considered above yield values small enough for us to conclude that lifetime broadening due to the scattering of excited carriers should be of little importance in determining the shape of the optical spectra.

IV. CONCLUSIONS

We have studied band gap renormalization in laser-excited GaAs. The cases we considered were those of intense excitation ($\sim 10\%$) in which excited electrons occupy the lowest-lying conduction states and the excited holes occupy the highest-lying valence states. The quasiparticle self-energy was computed with a non-equilibrium variant of the GW approximation using the Keldysh technique. Our study indicates that it is not possible to induce complete band gap closure by purely electronic means. In reaching this conclusion, we found that the contribution of the Hartree term to BGR, describing the mean-field interaction between an excited electron (or hole) and the charge density of the remaining electrons, is important and cannot be neglected. Our findings seem to support experimental observations⁷ in which no evidence of electronically-induced band gap closure was seen.

V. ACKNOWLEDGMENTS

C.D.S. would like to thank Dr. David J. Roundy for helpful discussions regarding the constrained LDA calculations. We also thank Dr. Eric K. Chang for his contributions to the early stages of this project. This work was supported by the NSF under Grant No. DMR0087088, and the Office of Energy Research, Office of Basic Energy Sciences, Materials Sciences Division of the U.S. Department of Energy (DOE) under Contract No. DE-AC03-76SF00098. Computer time was provided by the DOE at the Lawrence Berkeley National Laboratory (LBNL)'s NERSC center. Portions of this work were performed under the auspices of the DOE by University of California Lawrence Livermore National Laboratory (LLNL) under contract No. W-7405-Eng-48. Collaborations between LLNL and LBNL were facilitated by the DOE's Computational Materials Sciences Network.

Appendix

In this section, we present the Langreth rule¹⁵ for analytic continuation of *products* of functions integrated over contour C . This is necessary when evaluating the GW self-energy expression. The functions introduced in (6) satisfy

the Keldysh relation:

$$A^r(t, t') - A^a(t, t') = A^>(t, t') - A^<(t, t'), \quad (\text{A.1})$$

and also that for any functions A and B :

$$A^r(t, t')B^a(t, t') = A^a(t, t')B^r(t, t') = 0. \quad (\text{A.2})$$

The Langreth rule for analytic continuation states that if on the contour:

$$F = \int_C AB$$

then on the real time axis (for a concise derivation see¹⁶):

$$\begin{aligned} F^r &= \int_{-\infty}^{\infty} A^r B^r \\ F^a &= \int_{-\infty}^{\infty} A^a B^a \\ F^< &= \int_{-\infty}^{\infty} A^r B^< + A^< B^a \\ F^> &= \int_{-\infty}^{\infty} A^r B^> + A^> B^a. \end{aligned} \quad (\text{A.3})$$

It can also be shown that if:

$$\begin{aligned} F(\tau, \tau') &= A(\tau, \tau')B(\tau, \tau') \\ D(\tau, \tau') &= A(\tau, \tau')B(\tau', \tau), \end{aligned}$$

then:

$$F^r(t, t') = A^<(t, t')B^r(t, t') + A^r(t, t')B^<(t, t') + A^r(t, t')B^r(t, t'), \quad (\text{A.4})$$

and:

$$\begin{aligned} D^r(t, t') &= A^<(t, t')B^a(t', t) + A^r(t, t')B^<(t', t) \\ D^a(t, t') &= A^<(t, t')B^r(t', t) + A^a(t, t')B^<(t', t) \\ D^<(t, t') &= A^<(t, t')B^>(t', t) \\ D^>(t, t') &= A^>(t, t')B^<(t', t). \end{aligned} \quad (\text{A.5})$$

This result can be directly applied to the evaluation of the GW self-energy expression, where G and W replace A and B respectively (as well as to the polarizability P , replacing A and B by G).

- ¹ D.S. Chemla, *Semiconductors and Semimetals* **58**, 175 (1999), and references therein.
² H. Kalt and M. Rinker, *Phys. Rev. B* **45**, 1139 (1992).
³ L. Hedin and S. Lundqvist, *Solid State Phys.* **23**, 1 (1969).
⁴ M.S. Hybertsen and S.G. Louie, *Phys. Rev. B* **34**, 5390 (1986).
⁵ H. Haug and Schmitt-Rink, *Prog. Quant. Electr.* **9**, 3 (1984).
⁶ A. Oshlies, R.W. Godby, and R.J. Needs, *Phys. Rev. B* **51**, 1527 (1995).
⁷ L. Huang, J.P. Callan, E.N. Glezer, and E. Mazur, *Phys. Rev. Lett.* **80**, 185 (1998); J.P. Callan, A.M.T. Kim, L. Huang, and E. Mazur, *Chem. Phys.* **251**, 167 (2000). See also the review article, S.K. Sundrum and E. Mazur, *Nature Materials* **1**, 217 (2002).
⁸ J.S. Graves and R.E. Allen, *Phys. Rev. B* **58**, 13627 (1998).
⁹ L.X. Benedict, *Phys. Rev. B* **63**, 075202 (2001).
¹⁰ D.H. Kim, H. Erenreich, and E. Runge, *Sol. Stat. Com.* **89**, 119 (1994).
¹¹ The physics of electron-hole interaction is left out of this treatment since we focus our attention on the one-particle Green function. For a discussion of such two-particle effects in highly excited GaAs, see⁹.

- ¹² L.V. Keldysh, Sov. Phys. JETP **20**, 1018 (1965) [J. Exptl. Theoret. Phys. (U.S.S.R.) **47**, 1515 (1964)].
- ¹³ J. Rammer, Rev. Mod. Phys. **58**, 323 (1986).
- ¹⁴ In the equilibrium problem at $T=0$, in which one is interested in ground state expectation values, the contour can extend from $t = -\infty$ to $t = +\infty$ because the adiabatic turning-on and -off of the interaction is guaranteed to return the system to its (non-interacting) ground state. This is not true of excited states. For equilibrium problems with $T > 0$, the Wick rotation affected in the Matsubara treatment renders the problem essentially isomorphic to that of $T=0$. For a detailed discussion of equilibrium and non-equilibrium many-body perturbation theoretic techniques, see L.P. Kadanoff, and G. Baym *Quantum Statistical Mechanics* (W.A. Benjamin, Inc., New York, 1962).
- ¹⁵ D.C. Langreth *Linear and Nonlinear Electron Transport in Solids* edited by J.T. Devreese and E. Van Doren (Plenum, New York, 1976).
- ¹⁶ H. Haug and A.-P. Jauho *Quantum Kinetics in Transport and Optics of Semiconductors* (Springer, Berlin, 1996).
- ¹⁷ M. Hartmann, H. Stolz and R. Zimmerman, Phys. Stat. Sol. (B) **159**, 35 (1990).
- ¹⁸ W. Kohn and L.J. Sham, Phys. Rev. **140**, A1133 (1965).
- ¹⁹ L.X. Benedict, C.D. Spataru and S.G. Louie, Phys. Rev. B **66**, 085116 (2002).
- ²⁰ N. Troullier and J.L. Martins, Phys. Rev. B **43**, 1993 (1991).
- ²¹ H.J. Monkhorst and J.D. Pack, Phys. Rev. B **13**, 5188 (1976).
- ²² We stress that the occupation number distribution, $f(E)$ entering our calculation is assumed rather than calculated. In principle, $f(E)$ should be determined self-consistently, but the computational rigors of such a calculation preclude us from doing this here. The $f(E)$ is therefore an *input* to our calculation of band gap renormalization.
- ²³ At larger times, changes in the dielectric function were observed, and are believed to be signatures of a non-thermal structural transformation to a metallic amorphous state.

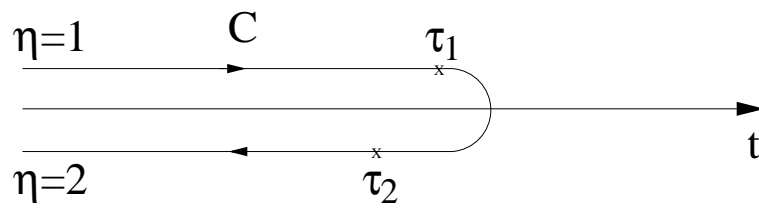


FIG. 1: Closed time path contour C along real axis, showing two branches, $\eta = 1, 2$.

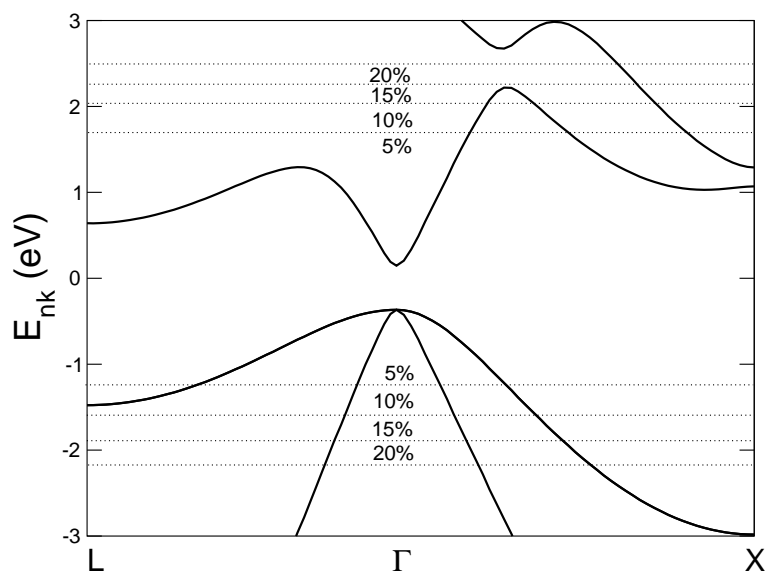


FIG. 2: Excited carrier occupation in GaAs; the LDA band structure shown here is taken from the unexcited case.

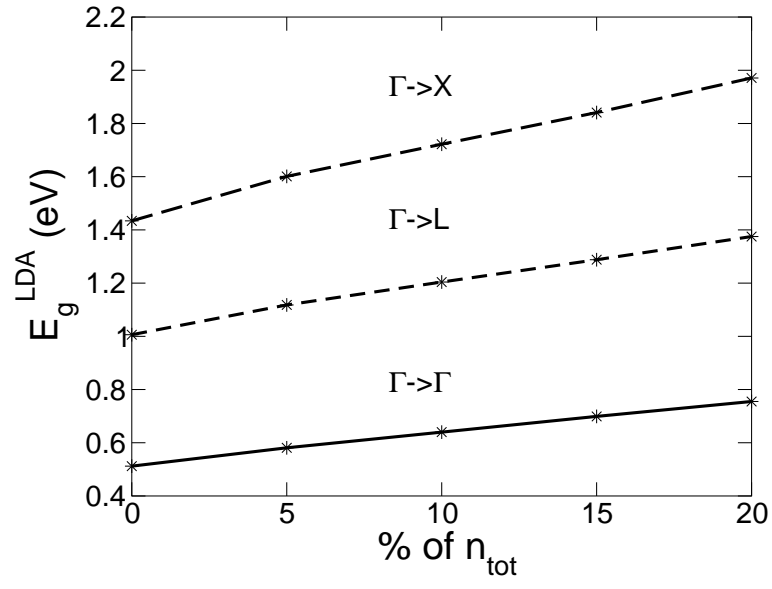


FIG. 3: Theoretical Kohn-Sham band gaps of GaAs calculated within the constrained LDA.

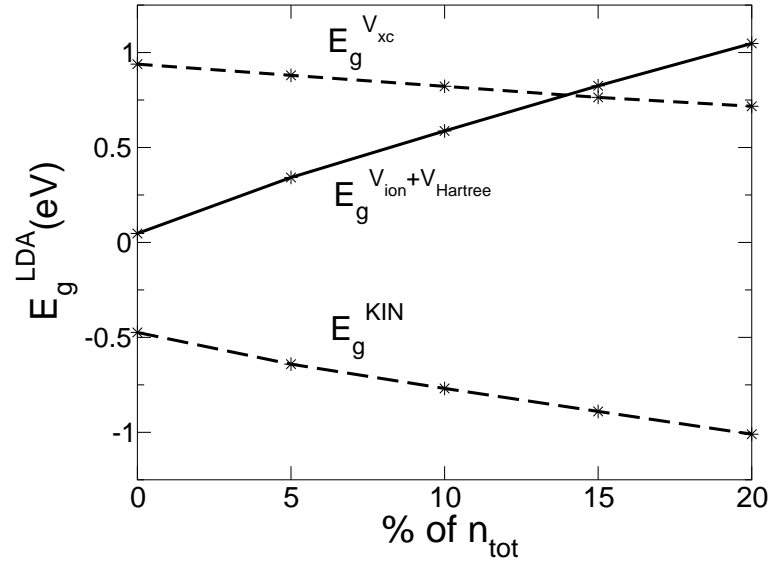


FIG. 4: Different contributions to Kohn-Sham band gap at Γ for GaAs calculated in the constrained LDA.

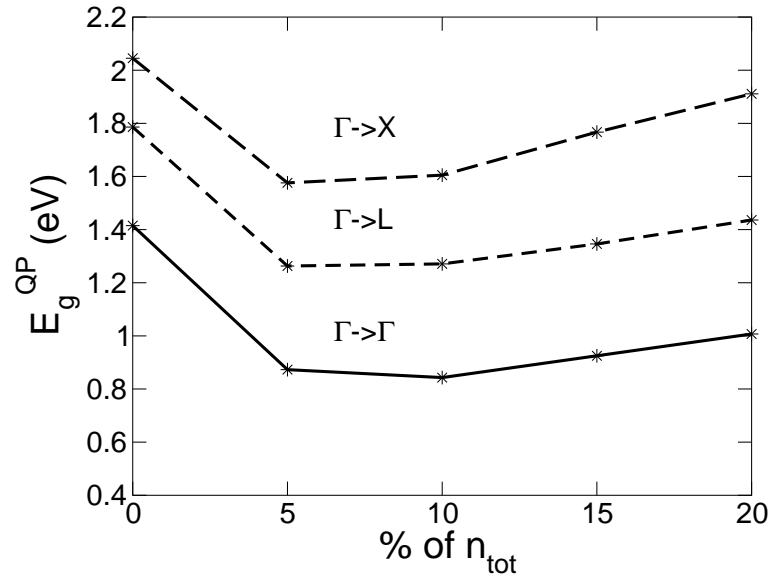


FIG. 5: The quasiparticle band gaps of GaAs as a function of excited carrier density calculated within the GW approximation.

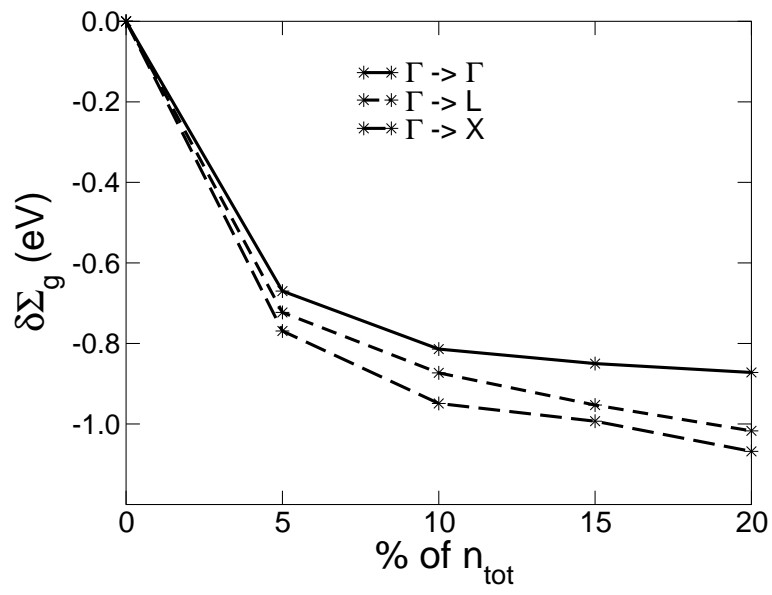


FIG. 6: Self-energy contribution to the band gap of GaAs as a function of excited carrier density.

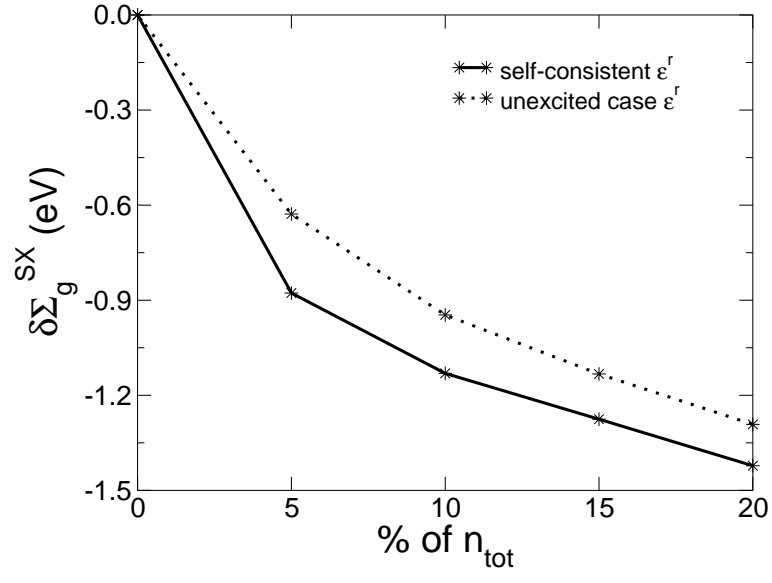


FIG. 7: Screened-exchange self-energy contribution to the band gap of GaAs at Γ as a function of excited carrier density.